

Coupling of denitrification and anaerobic ammonium oxidation with nitrification in sediments of the Yangtze Estuary: Importance and controlling factors



Cheng Liu^a, Lijun Hou^{a,*}, Min Liu^{b,c}, Yanling Zheng^{a,b,c}, Guoyu Yin^{b,c}, Ping Han^{a,b,c}, Hongpo Dong^a, Juan Gao^a, Dengzhou Gao^{b,c}, Yongkai Chang^a, Zongxiao Zhang^a

^a State Key Laboratory of Estuarine and Coastal Research, East China Normal University, Shanghai, 200241, China

^b Key Laboratory of Geographic Information Science (Ministry of Education), East China Normal University, Shanghai, 200241, China

^c School of Geographic Sciences, East China Normal University, Shanghai, 200241, China

ARTICLE INFO

Keywords:

Denitrification
Anammox
Sediment
Coupled nitrification-nitrogen removal processes
Yangtze estuary

ABSTRACT

Coupling of denitrification and anaerobic ammonium oxidation (anammox) with nitrification is an important mechanism for controlling nitrogen removal from aquatic ecosystems. In this work, we determined ambient rates of denitrification and anammox and their coupling links to nitrification in sediments of the Yangtze Estuary along a salinity gradient, using continuous-flow experiments combined with ¹⁵N isotope pairing technique. The rates of total denitrification and coupled nitrification-denitrification ranged from 0.44 to 7.03 $\mu\text{mol N m}^{-2} \text{h}^{-1}$ and from below the detection limit to 4.26 $\mu\text{mol N m}^{-2} \text{h}^{-1}$, respectively. The rates of total anammox and coupled nitrification-anammox varied from 0.09 to 1.21 $\mu\text{mol N m}^{-2} \text{h}^{-1}$ and from below the detection limit to 0.73 $\mu\text{mol N m}^{-2} \text{h}^{-1}$, respectively. It is shown that high availability of NO_3^- in bottom water as well as ferrous iron and organic carbon in sediments was beneficial to the uncoupled nitrogen removal processes, while low NO_3^- concentration in bottom water promoted the coupled nitrification-nitrogen removal processes. Along the salinity gradient, the coupled nitrification-nitrogen removal processes were the main nitrogen removal pathway in the Yangtze Estuary, and their contribution to total nitrogen removal was affected by NO_3^- concentrations, dissolved oxygen and salinity of sampling sites. Overall, this study improves the understanding of nitrate transformation processes in the estuarine and coastal environments.

1. Introduction

Nitrogen is an important element in controlling aquatic primary production (Falkowski et al., 1998). In the last few decades, human activities have contributed to excessive input of artificial nitrogen into aquatic environments mainly through widespread use of nitrogen fertilizers and combustion of fossil fuels (Galloway et al., 1996). Increased nitrogen loading triggers severe environmental and ecological issues (e.g., eutrophication, hypoxia and harmful algae bloom) of aquatic ecosystems, especially estuarine and coastal environments (Paerl and Fulton, 2006). Therefore, an understanding of nitrogen transformation processes and associated underlying mechanisms is required for the development of management strategies in controlling aquatic nitrogen pollution.

Denitrification and anaerobic ammonium oxidization (anammox) are of particular interest because they can convert nitrate and/or nitrite

to di-nitrogen gas. Both processes thus remove permanently reactive nitrogen from aquatic environments and counteract the detrimental effects caused by nitrogen overload (Yin et al., 2015). Numerous studies have documented that these two nitrogen transformation processes are associated tightly with environmental factors such as temperature, salinity, dissolved oxygen (DO) and nutrients of overlying water, and organic matter, sulfide, metal oxides, particle size of sediment (Burgin and Hamilton, 2007; Minjeaud et al., 2008; Jha and Minagawa, 2013; Fernandes et al., 2016; Jia et al., 2016; Marks et al., 2016; Zheng et al., 2016; Xia et al., 2017). With the development and application of stable isotope analysis techniques, the denitrification process has been further clarified. For example, by using the nitrogen isotope pairing technique, Nielsen (1992) discriminated between denitrification of nitrate derived from the overlying water, which is defined as uncoupled denitrification (or called direct denitrification, D_w) and denitrification of nitrate from nitrification, which is defined as coupled nitrification-denitrification

* Corresponding author.

E-mail address: ljhou@sklec.ecnu.edu.cn (L. Hou).

<https://doi.org/10.1016/j.ecss.2019.02.043>

Received 18 June 2018; Received in revised form 12 February 2019; Accepted 18 February 2019

Available online 23 February 2019

0272-7714/ © 2019 Elsevier Ltd. All rights reserved.

(D_n). However, occurrence of anammox is a challenge to the isotope pairing technique, because it leads to violation of the assumption that produced $^{28}\text{N}_2$, $^{29}\text{N}_2$, and $^{30}\text{N}_2$ are binomially distributed (Mulder et al., 1995). To accurately distinguish D_w and D_n , Risgaard-Petersen et al. (2003) improved Nielsen's isotope pairing method, by which di-nitrogen gas originated from anammox is separated from denitrification. Through the above methods, the rates of D_w and D_n in different aquatic environments (such as lake, river, estuary, and coastal shelf) were determined (Seitzinger et al., 2006). Like coupled nitrification-denitrification, a possible coupling between nitrification and anammox can be envisaged. This hypothesis is strengthened by the finding that both denitrification and anammox coupled with nitrification co-occurred in certain conditions (Strous, 2000; Jetten et al., 2001; Lindsay et al., 2001). Coupling of denitrification and anammox with nitrification is thus an important mechanism for nitrogen removal from aquatic ecosystems. Current research has focused mainly on spatial and temporal distributions of these processes, however exact factors controlling these processes remain unclear for a specific aquatic environment.

The Yangtze Estuary is the largest estuary in China, connecting the Yangtze River with the East China Sea. Under the interaction between river runoff and tidal current, there are great gradient variations in physical, chemical, and biological factors along the estuary (Bo et al., 2009; Deng et al., 2015). In addition, the Yangtze Estuary is situated in one of the most densely populated regions of China. Over the past several decades, large amounts of anthropogenic nitrogen from the Yangtze River basin have been discharged into the estuarine and coastal region, consequently causing severe eutrophication and harmful algal blooms (Hou et al., 2013; Zheng et al., 2014). Nitrogen pollution has thus been identified as the most serious environmental issue in the Yangtze Estuary and its adjacent area (Hou et al., 2015a,b; Yin et al., 2017; Zheng et al., 2017). So far, to our knowledge, potential rates of both denitrification and anammox have been extensively examined in sediments of the Yangtze Estuary using sediment-slurry incubation experiments (Hou et al., 2013; Song et al., 2013; Deng et al., 2015; Lin et al., 2017), however few studies have addressed the ambient rates of both denitrification and anammox and their coupling with nitrification. In the present study, we conducted continuous-flow experiments combined with ^{15}N isotope pairing technique to investigate coupled nitrification-denitrification/anammox along the Yangtze Estuary. The purposes of this study are (1) to determine ambient rates of denitrification and anammox in the Yangtze estuarine sediments, (2) to elucidate coupling links of denitrification/anammox with nitrification, and (3) to reveal key factors affecting the relative importance of coupled nitrification-nitrogen removal processes. This study provides new insights into nitrate transformation dynamics in the Yangtze estuarine and coastal ecosystem.

2. Materials and methods

2.1. Sample collection

Samples were collected aboard “Runjiang 1” scientific expedition vessel from 7 sites along the Yangtze Estuary in winter (February) and summer (July) of 2017 (Fig. 1). At each site, six intact sub-cores (7.0 cm diameter and 15 cm deep) were retrieved, using a box corer which preserved the integrity of the sediment-water interface. Meanwhile, 30 L of near-bottom water were taken from each site for nutrient analyses and continuous-flow experiments. Three sub-cores were used for the continuous-flow experiments, while surface sediment (0–5 cm deep) of the remaining sub-cores was mixed to produce one composite sample under a helium atmosphere for slurry experiments and analyses of sediment physicochemical characteristics.

2.2. Continuous-flow experiments

Three intact sediment cores from each site were installed

respectively into a gas-tight continuous-flow system (Hou et al., 2012; Yin et al., 2016). Specifically, each core was wrapped with aluminum foil to keep the incubation dark. An acetol plunger with a Viton o-ring was inserted into each core to ~ 5 cm above the sediment-water interface, which left the overlying water of about 230 mL within each core. Polyetheretherketone (PEEK) tubing connected the inlet port of each plunger to unfiltered bottom water via a multi-channel peristaltic pump and the outlet port to a sample collection vial. The bottom water, enriched with $^{15}\text{N-NO}_3^-$ (90–99% $^{15}\text{N-KNO}_3$) to final concentrations of 100 μM $^{15}\text{N-NO}_3^-$ and kept at near *in situ* temperature and dissolved oxygen (Minjeaud et al., 2008; Yin et al., 2015), was pumped through the continuous-flow system at a flow rate of 1.0–1.4 mL min^{-1} (Gardner and McCarthy, 2009). After an initial overnight pre-incubation to allow the experimental system to reach equilibrium (Mctigue et al., 2016), inflow and outflow water for analyses of dissolved nitrogen gases ($^{29}\text{N}_2$ and $^{30}\text{N}_2$) were taken with gas-tight vials (12 mL Exetainer, Labco, High Wycombe, UK) by allowing vials to overflow from the bottom three times, ensuring that no air bubbles were captured. These samples were collected once every 24 h for 4 days. After collection, each sample was injected with 200 μL 50% ZnCl_2 solution to inhibit microbial activity, and all Exetainer vials were sealed with butylrubber septa and stored underwater at 4 °C until analysis. In this study, concentrations of dissolved nitrogen gas were measured by membrane inlet mass spectrometry (HPR-40, Hiden Analytical, UK), with a detection limit of 0.1 $\mu\text{mol N}_2 \text{ L}^{-1}$ (An and Gardner, 2002; Tortell, 2005; Yin et al., 2014).

2.3. Calculation of denitrification and anammox rates

Denitrification rates of $^{15}\text{NO}_3^-$ (D_{15}) and $^{14}\text{NO}_3^-$ (D_{14} , referred to as ambient denitrification rate) were calculated by the following equations (Risgaard-Petersen et al., 2003; Trimmer et al., 2006):

$$D_{15} = 2 \times p^{30}\text{N}_2 \times (1 + r_{14}) \quad (1)$$

$$D_{14} = D_{15} \times r_{14} \quad (2)$$

where $p^{30}\text{N}_2$ ($\mu\text{mol N m}^{-2} \text{ h}^{-1}$) is the total measured $^{30}\text{N}_2$ production rate, and r_{14} is the ratio of $^{14}\text{NO}_3^-$ to $^{15}\text{NO}_3^-$ undergoing nitrate reduction. The r_{14} was estimated from the contribution of anammox to the total production of N_2 (r_a) measured within anaerobic slurry experiments (Supporting Information), as follows:

$$r_{14} = ((1-r_a) \times R_{29-r_a}) / (2-r_a) \quad (3)$$

where R_{29} is the ratio of $p^{29}\text{N}_2$ to $p^{30}\text{N}_2$, and $p^{29}\text{N}_2$ ($\mu\text{mol N m}^{-2} \text{ h}^{-1}$) is the total measured $^{29}\text{N}_2$ production rate. D_w and D_n rates were then calculated by the following equations:

$$D_w = D_{15} \times [^{14}\text{NO}_3^-] / [^{15}\text{NO}_3^-] \quad (4)$$

$$D_n = D_{14} - D_w \quad (5)$$

Here, the concentration of $^{14}\text{NO}_3^-$ was determined from ambient bottom water, and $^{15}\text{NO}_3^-$ was determined as the difference between the total NO_3^- concentration after addition of $^{15}\text{NO}_3^-$ tracer and its ambient level (Yin et al., 2015).

The supply of NO_2^- is a key regulator of anammox. NO_2^- could be supplied from overlying water, NO_3^- reduction by anaerobic denitrification, or oxidation of NH_4^+ to NO_2^- by aerobic nitrification (Meyer et al., 2005). Numerous studies reported that in some nitrite-limited aquatic environments, intermediate products of denitrification and nitrification are the main sources of NO_2^- (Trimmer et al., 2003; Meyer et al., 2005; Yoshinaga et al., 2011; Zhou et al., 2014). Low NO_2^- level was also detected in bottom water of the Yangtze Estuary (Hou et al., 2013). Therefore, NO_2^- produced by denitrification and nitrification was regarded as the dominant supply to anammox in the present study. We calculated anammox rate of $^{15}\text{NO}_2^-$ (A_{15}) and $^{14}\text{NO}_2^-$ (A_{14} , referred to as ambient anammox rate), anammox rate of

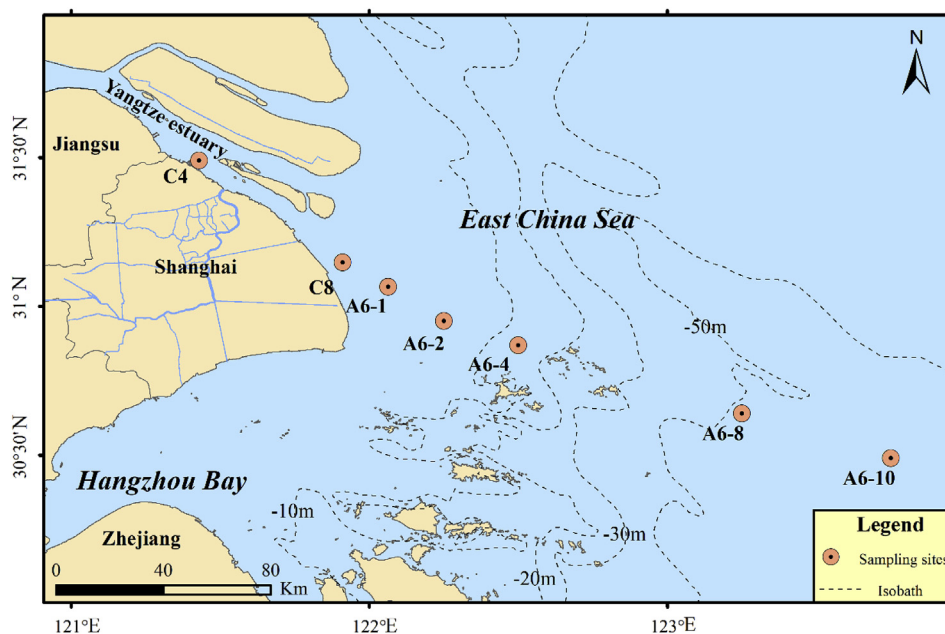


Fig. 1. Map of the Yangtze Estuary, showing sampling sites.

nitrite from the intermediate product of D_w (A_w , called uncoupled anammox), and anammox rate of nitrite from the intermediate product of nitrification (A_n , called coupled nitrification-anammox), respectively, according to the following equations:

$$A_{15} = p^{29}N_2 \cdot 2 \times r_{14} \times p^{30}N_2 \tag{6}$$

$$A_{14} = A_{15} \times r_{14} \tag{7}$$

$$A_w = A_{15} \times [^{14}NO_3^-] / [^{15}NO_3^-] \tag{8}$$

$$A_n = A_{14} - A_w \tag{9}$$

2.4. Determination of environmental parameters

Depth and temperature were measured *in situ* with CTD. After bottom water samples were collected, salinity, pH, and dissolved oxygen (DO) were measured immediately using YSI-30 portable salinity meter, ALALIS pH 400 pH meter, and YSI-550A portable DO meter, respectively. Concentrations of nutrients in bottom water were determined by a continuous-flow nutrient analyzer (SAN Plus, Skalar Analytical B.V., the Netherlands), with detection limits of 0.5 μM for ammonium and 0.1 μM for nitrate and nitrite (Gao et al., 2017). Organic carbon (OC) was determined with a carbon-hydrogen-nitrogen elementary analyzer (VVarioELIII) after leaching with 0.1 M HCl to remove sedimentary carbonate (Lin et al., 2017). Readily oxidizable

organic carbon (ROOC) was determined using potassium permanganate method (Shang et al., 2011). Content of Fe (II) was quantified after extraction with 0.5 M HCl from fresh sediments, followed by colorimetric (Ferrozine) analysis (Roden and Lovley, 1993). Sediment sulfide concentration was analyzed using an Orion Sure-flow[®] combination silver-sulfide electrode, with a detection limit of 0.09 μM (Hou et al., 2012). Grain size of sediment was measured using a LS 13320 Laser Grain Sizer.

2.5. Data analysis

Analysis of variance (ANOVA) was performed to examine temporal and spatial differences in different denitrification rates (D_{14} , D_w , and D_n) and anammox rates (A_{14} , A_w , and A_n). Correlations of environment variables with ambient rates of D_{14} and A_{14} were analyzed with Pearson's correlation. The above statistical analyses were conducted using Statistical Package of Social Sciences (SPSS, version-22.0). Redundancy analysis (RDA) was performed to reveal the effects of environment variables on D_w , D_n , A_w and A_n , as well as their relative importance in total nitrogen removal. The RDA analysis was conducted using CANOCO 5.

Table 1
Physicochemical characteristics of near-bottom water from the sampling sites.

Stations	C4		C8		A6-1		A6-2		A6-4		A6-8		A6-10	
	Feb.	Jul.	Feb.	Jul.	Feb.	Jul.	Feb.	Jul.	Feb.	Jul.	Feb.	Jul.	Feb.	Jul.
Depth (m)	10	9	9	8	6	8	9	9	17	16	61	59	56	54
TEMP (°C)	12.5	25.3	9.9	24.2	11.3	25.9	8.9	24.5	8.8	22.0	14.4	19.1	14.0	21.2
SAL	0.2	0.2	6.7	0.6	20.0	4.5	24.0	13.3	30.7	26.7	35.8	29.5	35.4	32.6
pH	7.97	7.79	8.00	7.88	7.94	7.72	7.95	7.88	8.08	7.91	8.07	7.90	8.05	7.95
DO (mg L ⁻¹)	11.31	5.65	11.13	5.28	10.85	6.30	10.58	6.77	10.61	4.80	8.55	4.04	8.77	4.39
NO ₃ ⁻ (μM)	138.2	94.11	117.41	107.02	58.16	91.14	48.65	53.51	19.95	26.98	3.31	10.35	4.26	7.55
NO ₂ ⁻ (μM)	2.42	0.11	1.55	1.21	0.24	0.35	0.22	1.01	0.16	1.45	0.14	0.36	0.23	0.52
NH ₄ ⁺ (μM)	1.65		11.60		4.26	1.33	4.26	3.59	4.55	5.52	4.53	6.93	4.17	6.71

TEMP: temperature; SAL: salinity; DO: dissolved oxygen; denotes that the value is under the detection limit.

3. Results

3.1. Site characteristics

Sampling sites ranged between depths of 6–61 m (Table 1). Benthic water temperature in July was higher than that in February, with the respective ranges of 19.1–25.9 °C and 8.8–14.4 °C. Salinity of benthic water ranged from 0.2 to 35.8 in February and from 0.2 to 32.6 in July. The salinity in February was higher than that in July, especially at the mid-estuary stations (C8, A6-1 and A6-2). Benthic water pH varied from 7.94 to 8.08 in February and from 7.72 to 7.95 in July. DO contents in benthic water ranged from 8.55 to 11.31 mg L⁻¹ in February. In contrast, they were relatively lower in July, with values of 4.04–6.77 mg L⁻¹. A strong negative correlation was observed between DO and temperature (Table S1). Nitrate concentrations in benthic water had a large gradient change along the estuary, ranging from 3.31 to 138.20 μM in February and from 7.55 to 107.02 μM in July. The concentrations of nitrate were negatively related to salinity (Table S1). Nitrite concentrations in benthic water were relatively low in the study area, with values of 0.14–2.42 μM in February and from 0.11 to 1.45 μM in July. A positive correlation was observed between nitrite and nitrate concentrations (Table S1). Ammonium concentrations in benthic water varied from 1.65 to 11.60 μM in February and from below the detection limit to 6.93 μM in July. Generally, the concentrations of ammonium increased seawards along the estuarine gradient.

Sediments of sampling sites were characterized by sand-silt, with clay (< 4 μm), silt (4–63 μm), and sand (> 63 μm) contents accounting for about 1.9–9.1%, 25.0–91.6%, and 0.4–71.0% of the total sediments, respectively (Table 2). Sediment median grain size in the study area ranged from 8.7 to 117.1 μm, showing a large spatial variation. Water contents of sediment varied from 23.4 to 45.1% in February and from 25.1 to 46.2% in July, which were closely related to sediment grain sizes (Table S1). Contents of sedimentary ferrous iron ranged from 0.77 to 1.93 mg g⁻¹ in February and from 0.27 to 2.89 mg g⁻¹ in July. Concentrations of sulfide in sediments varied from 0.1 to 9.2 μmol L⁻¹ in February and from below the detection limit to 7.1 μmol L⁻¹ in July. Contents of organic carbon in sediments were higher in July (2.97–13.02 mg g⁻¹) than in February (1.02–8.58 mg g⁻¹). Generally, the concentrations of ferrous iron, sulfide and OC were correlated positively to the proportions of both clay and silt, but negatively to the proportion of sand (Table S1). Concentrations of ROOC in February (0.24–0.88 mg g⁻¹) were comparable to those in July (0.25–0.97 mg g⁻¹). Also, ROOC concentrations were related positively to concentrations of ferrous iron and sulfide (Table S1).

3.2. Ambient rates of denitrification and anammox

D₁₄ rates ranged from 1.43 to 5.47 μmol N m⁻² h⁻¹ in February and from 0.44 to 7.03 μmol N m⁻² h⁻¹ in July (Fig. 2a). A significant spatial difference in the D₁₄ rates was observed among the sampling

Table 2
Physicochemical characteristics of sediments from the sampling sites.

Stations	C4		C8		A6-1		A6-2		A6-4		A6-8		A6-10	
	Feb.	Jul.	Feb.	Jul.	Feb.	Jul.								
Water content (%)	38.2	25.5	37.0	36.5	45.1	46.2	42.7	43.1	40.1	39.9	23.4	26.9	23.4	25.1
Clay (%)	2.8	1.9	7.6	7.7	4.6	7.4	6.7	9.1	7.9	8.6	4.8	7.1	4.0	3.7
Silt (%)	58.0	36.7	85.3	81.8	87.3	91.6	89.4	90.5	89.8	90.2	38.5	62.2	25.0	35.7
Sand (%)	39.2	61.4	7.1	10.4	8.1	1.0	4.0	0.4	2.3	1.2	56.7	30.7	71.0	60.6
MΦ (μm)	34.7	115.4	8.7	9.6	11.2	10.2	20.3	8.8	10.6	9.4	104.7	10.7	117.1	91.8
Fe ²⁺ (mg g ⁻¹)	1.14	0.27	1.93	2.89	0.90	1.14	1.07	1.23	1.21	1.20	1.35	0.85	0.77	0.77
Sulfide (μmol L ⁻¹)	0.2	0.6	3.2	3.3	1.2	4.0	2.2	3.1	9.2	7.1	2.2	0.1	0.1	0.9
OC (mg g ⁻¹)	5.08	2.97	8.58	10.63	6.03	10.47	5.86	13.02	1.02	12.22	2.42	4.59	5.40	3.94
ROOC (mg g ⁻¹)	0.24	0.29	0.82	0.83	0.52	0.97	0.57	0.88	0.88	0.83	0.65	0.29	0.38	0.25

MΦ: median grain size; OC: organic carbon; ROOC: readily oxidizable organic carbon; denotes that the value is under the detection limit.

sites (one-way ANOVA, n = 21, p < 0.05 for February; one-way ANOVA, n = 21, p < 0.01 for July). In February, the highest D₁₄ rate appeared at site A6-4, and the lowest D₁₄ rate at site A6-10. In July, the highest D₁₄ rate also occurred at site A6-4, and the lowest D₁₄ rate at site C4. However, no significant temporal variation in the D₁₄ rates was detected in the entire study area (one-way ANOVA, n = 42, p > 0.05). The D₁₄ rates were correlated positively with sulfide concentrations, ROOC, and clay contents of sediment in the Yangtze Estuary (Table S1).

A₁₄ rates ranged from 0.09 to 0.53 μmol N m⁻² h⁻¹ and from 0.14 to 1.21 μmol N m⁻² h⁻¹ in February and July, respectively (Fig. 3-a). A significant spatial difference in the A₁₄ rates was observed among the sampling sites (one-way ANOVA, n = 21, p < 0.05 for February; one-way ANOVA, n = 21, p < 0.01 for July). In February, the highest A₁₄ rate appeared at site C8, and the lowest A₁₄ rate at site A6-10. In July, the highest A₁₄ rate occurred at site A6-4, and the lowest rate at site C4. Meanwhile, a significant seasonal variation in the A₁₄ rates was observed (one-way ANOVA, n = 42, p < 0.01). In general, the A₁₄ rates were higher in July than in February at all sampling sites, except for sites C4 and A6-2. The A₁₄ rates were correlated positively with sediment OC and D₁₄ rates in the Yangtze Estuary (Table S1).

3.3. D_w compared to D_n

Di-nitrogen gas production resulting from D_w and D_n was measured. The D_w rates ranged from 0.20 to 3.12 μmol N m⁻² h⁻¹ and from 0.44 to 4.47 μmol N m⁻² h⁻¹ in February and July, respectively (Fig. 2-b). The D_w rates showed a significant spatial variation in the study area (one-way ANOVA, n = 21, p < 0.05 for February; one-way ANOVA, n = 21, p < 0.01 for July). In general, the sampling sites with high nitrate concentrations (C4 and C8) had relatively great D_w rates, followed by the sampling sites with medium nitrate concentrations (A6-1, A6-2 and A6-4), and relatively low D_w rates were observed at the sampling sites with low nitrate concentrations (A6-8 and A6-10). The seasonal variation in the D_w rates was significant in the Yangtze Estuary (one-way ANOVA, n = 42, p < 0.05). The D_w rates were relatively higher in July than in February, except for site C4. The D_n rates ranged from 0.17 to 4.08 μmol N m⁻² h⁻¹ and from below the detection limit to 4.26 μmol N m⁻² h⁻¹ in February and July, respectively (Fig. 2-c). The D_n rates showed a significant spatial variation in the study area (one-way ANOVA, n = 21, p < 0.01 for both February and July). Generally, with the decrease of nitrate concentrations, the D_n rates increased seawards along the Yangtze Estuary. However, there was no significant seasonal variation in the D_n rates in the entire study area (one-way ANOVA, n = 42, p > 0.05).

3.4. A_w compared to A_n

Spatial and seasonal variations in A_w and A_n rates are shown in Fig. 3. The A_w rates ranged from 0.01 to 0.38 μmol N m⁻² h⁻¹ and from 0.09 to 0.62 μmol N m⁻² h⁻¹ in February and July, respectively. A

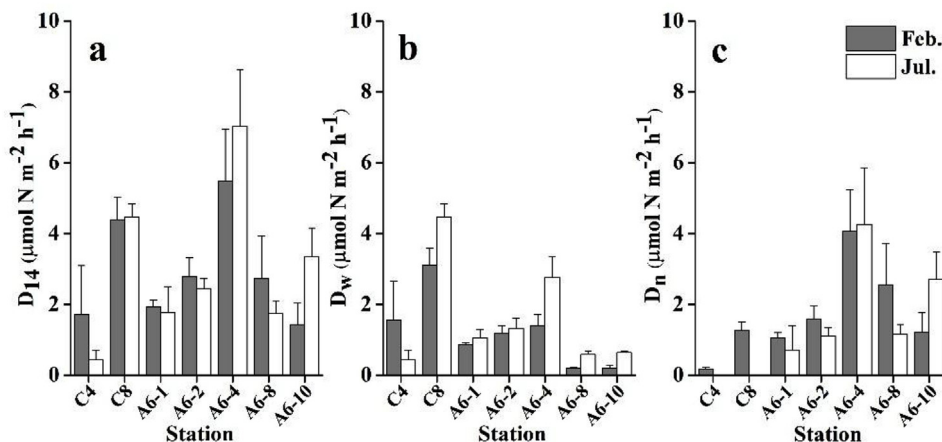


Fig. 2. Rates of denitrification of $^{14}\text{NO}_3^-$ (D_{14} , a), D_{14} fueled by bottom water $^{14}\text{NO}_3^-$ (D_w , b), and D_{14} fueled by nitrification-derived $^{14}\text{NO}_3^-$ (D_n , c) along the Yangtze Estuary in February and July. Bars denote the standard error of triplicate samples.

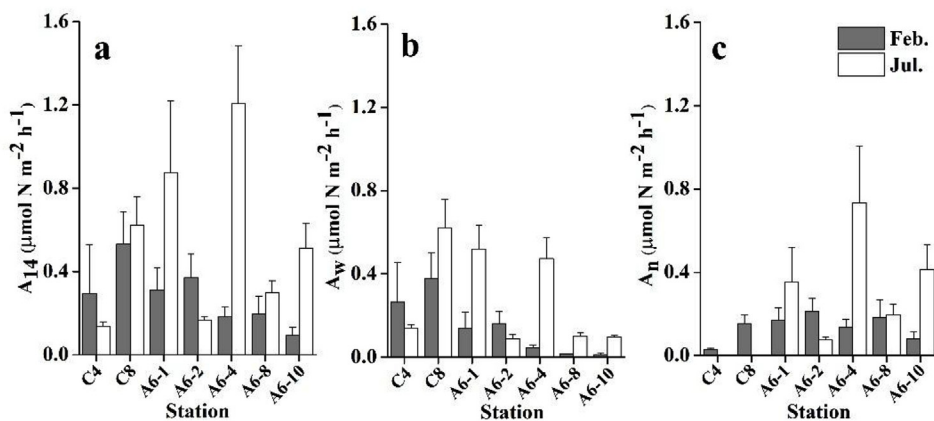


Fig. 3. Rates of anammox of $^{14}\text{NO}_2^-$ (A_{14} , a), A_{14} fueled by D_w -derived $^{14}\text{NO}_2^-$ (A_w , b), and A_{14} fueled by nitrification-derived $^{14}\text{NO}_2^-$ (A_n , c) along the Yangtze Estuary in February and July. Bars denote the standard error of triplicate samples.

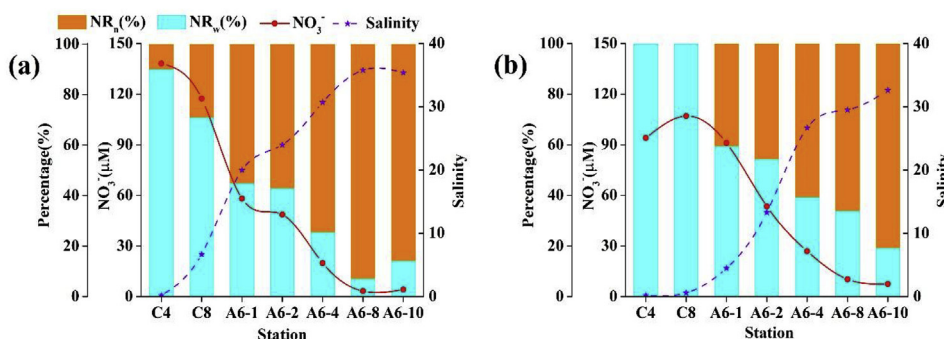


Fig. 4. Changes in nitrate, salinity and percentage of nitrogen removal relying on $^{14}\text{NO}_x^-$ from bottom water (NR_w) and nitrification (NR_n) in February (a) and July (b).

significant spatial difference in the A_w rates was observed among the sampling sites (one-way ANOVA, $n = 21$, $p < 0.01$ for both February and July). In February, with the decrease of nitrate concentrations, the A_w rates decreased seawards in the study area. In July, although there was no significant spatial difference in the A_w rates, the high A_w rate was observed at the site with high nitrate concentration (C8), the low A_w rate at the sites with relatively low nitrate concentrations (A6-8 and A6-10). There was a significant seasonal variation in the A_w rates (one-way ANOVA, $n = 42$, $p < 0.01$). The A_w rates were much higher in July than in February, except for sites C4 and A6-2. In this study, the A_w and D_w rates had similar spatial and seasonal variations. The A_n rates ranged from 0.03 to 0.21 $\mu\text{mol N m}^{-2} \text{ h}^{-1}$ and from below the

detection limit to 0.73 $\mu\text{mol N m}^{-2} \text{ h}^{-1}$ in February and July, respectively. A significant spatial difference in the A_n rates was observed among the sampling sites (one-way ANOVA, $n = 21$, $p < 0.05$ for February; one-way ANOVA, $n = 21$, $p < 0.01$ for July). A marked seasonal variation was also found for the A rates (one-way ANOVA, $n = 42$, $p < 0.01$). In February, the A rates at all sampling sites were identical. However, in July, with the decrease of nitrate concentrations, the A rates increased seawards, which was similar to the change of D_n rates.

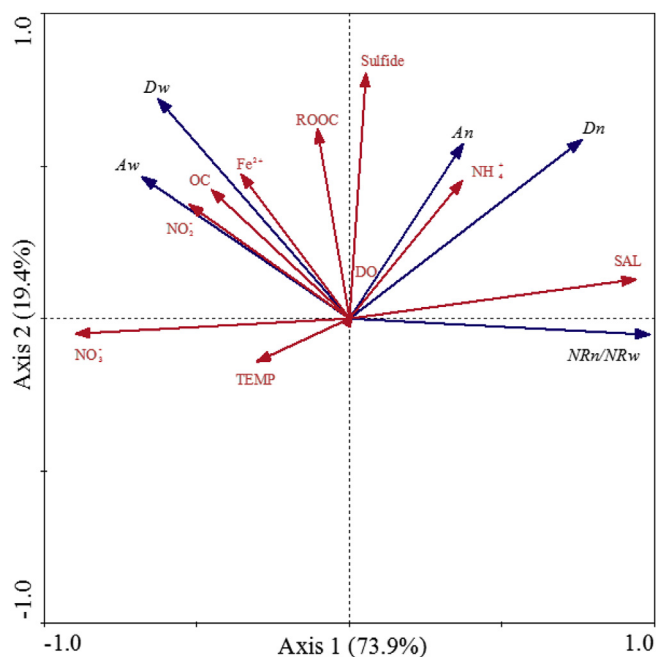


Fig. 5. RDA analysis of environment variables with the rates of denitrification relying on $^{14}\text{NO}_3^-$ from bottom water (D_w) and nitrification (D_n), the rates of anammox relying on $^{14}\text{NO}_2^-$ from product of D_w (A_w) and nitrification (A_n), and the ratios of nitrogen removal pathways relying on $^{14}\text{NO}_x^-$ from nitrification (NR_n) and bottom water (NR_w). SAL: salinity; DO: dissolved oxygen; ROOC: readily oxidizable organic carbon; OC: organic carbon; TEMP: temperature.

3.5. The percentage of different nitrogen removal processes

Nitrogen removal (NR, sum of denitrification and anammox) occurs relying on $^{14}\text{NO}_x^-$ from bottom water (NR_w , sum of D_w and A_w) and (or) from nitrification (NR_n , sum of D_n and A_n). The percentage of NR_w and (or) NR_n in the total NR can reflect the relative importance of these two different processes. In the present study, the percentages of NR_w in the total NR ranged from 7.2 to 90.1% and from 19.2 to 100% in February and July, respectively (Fig. 4). As shown in Fig. 4, with the decreasing nitrate concentrations and increasing salinity, the percentages of NR_w decreased in both February and July, while the percentages of NR_n increased. The relative importance of NR_w was greater in February than in July, while an opposite seasonal pattern was observed for the relative importance of NR_n .

RDA analysis was conducted to determine the correlations of different nitrogen removal pathways with environment variables (Fig. 5). The first two RDA axes (principal components) explained 93.3% of the cumulative percentage variance. The first and second axes accounted for 73.9% and 19.4% of the total variations in the rates of different denitrification and anammox pathways and the ratios of NR_n to NR_w , respectively. It is shown that NO_3^- , Fe^{2+} , OC and salinity were significantly correlated with the rates of different denitrification and anammox pathways and the ratios of NR_n to NR_w .

4. Discussion

4.1. Ambient rates of denitrification and anammox along the Yangtze Estuary

Denitrification and anammox are important mechanisms eliminating reactive nitrogen from aquatic environments (Dong et al., 2009; Crowe et al., 2012). The ambient rates of denitrification (D_{14}) and anammox (A_{14}) measured in this study were similar to those from the East China Sea (Song et al., 2013). Denitrification contributed 85–97%

and 67–94% of total nitrogen removal (sum of D_{14} and A_{14}) in February and July, respectively, while anammox contributed 3–15% and 6–33% of total nitrogen removal in February and July, respectively (Figs. 2 and 3). It shows that denitrification was the dominant pathway removing nitrogen from the Yangtze Estuary, compared with anammox. Previous studies have also revealed the importance of denitrification in nitrogen loss from estuarine and coastal sediments (Crowe et al., 2012; Song et al., 2013; Deng et al., 2015). In addition, according to the research conducted by Fernandes et al. (2016), the contribution of anammox to total nitrogen removal could reach up to 45%. Our results are thus in agreement with these previous studies.

The D_{14} rates showed significant spatial variations within the Yangtze Estuary. In both February and July, the highest D_{14} rate appeared at site A6-4 where sulfide was relatively enriched. As a reducing substance, sulfide can donate electron for nitrate, nitrite and N_2O reduction during the denitrification. Therefore, increased concentration of sulfide in sediment can promote denitrification (Aelion and Warttinger, 2010; Deng et al., 2015; Yang et al., 2015). In contrast, the sediments of sites A6-4 and C4 showed lower D_{14} rates in February and July, respectively, which may be due to low sedimentary sulfide contents. The assumption is also supported by the positive correlation between D_{14} rates and sulfide concentrations. On the contrary, some studies have shown that sulfide can slow down denitrification rate by inhibiting the metabolism of microorganisms (Brunet and Garcia-Gil, 1996; Senga et al., 2006; Aelion and Warttinger, 2010). This comparison implies that the site-specific effects of sulfide on denitrification may be related to contents and forms of sulfide (Burgin and Hamilton, 2007).

Numerous studies have reported that organic matter can favor the growth of heterotrophic denitrifying bacteria, and thus increase the denitrification activity (Piña-Ochoa and Álvaerz, 2006). However, the D_{14} rates were not correlated with OC in this study, which may be due to the bioavailability of OC (Dodla et al., 2008). In general, the OC with high bioavailability is more favorable to denitrification. This is also evidenced by the positive correlation of D_{14} rates with denitrification. As a labile fraction of OC, ROOC is relatively easily utilized by denitrification bacteria (Burgin and Hamilton, 2007). Therefore, both quantity and quality of OC are important factors affecting denitrification. Compared to coarse sediments, fine sediments were generally characterized by the relative high organic matter contents, which fuels microbial activity and nutrient regeneration (Jia et al., 2016; Xia et al., 2017). It might be an important reason for the observed positive correlation between D_{14} rates and clay contents.

Generally, the A_{14} rates were higher in July than in February, except for sites C4 and A6-2. In July, the near-bottom water temperature of each sampling site fell in the optimal temperature range (10–30 °C) for the activity of anammox bacteria (Awata et al., 2013). It probably explains the relatively higher A_{14} rates in July. In addition, the A_{14} rates were observed to positively correlate with the D_{14} rates (Table S1). This correlation reflects that anammox is coupled to denitrification which provides nitrite substrate for anammox (Zhou et al., 2014; Hou et al., 2015a,b; Zhao et al., 2015; Gao et al., 2017). As known, anammox is an autotrophic process in which OC is not required. Under high OC concentrations, anammox activity may be inhibited, because anammox bacteria are less competitive for nitrite compared with other heterotrophic microorganisms (Chamchoi et al., 2008). In this study, we found that the A_{14} rates were not related to sediment ROOC but to OC (Table S1). These relationships indicate that the composition of organic matter might also be a factor mediating sediment anammox, however more work is required to reveal the underlying mechanisms.

4.2. Different nitrogen removal processes along the Yangtze Estuary

In sediments, denitrifying and anammox bacteria require NO_3^- and/or NO_2^- as substrates that can derive either from overlying water (D_w and A_w) or from nitrification (D_n and A_n). In the present study, D_w ,

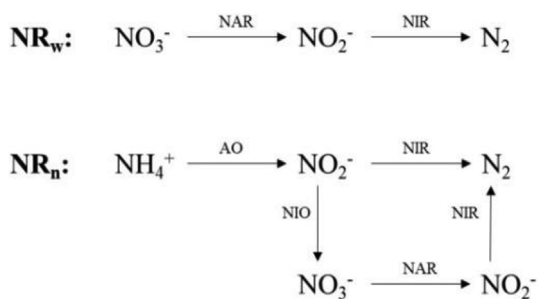


Fig. 6. Main pathways of nitrogen removal relying on $^{14}\text{NO}_x^-$ from bottom water (D_w and A_w) or nitrification (D_n and A_n). NAR: nitrate reduction; NIR: nitrite reduction; AO: ammonia oxidation; NIO: nitrite oxidation.

D_n , A_w , and A were discriminated on the basis of continuous-flow experiments combined with nitrogen isotope tracing technique. The results showed that D_w and D_n (as well as A_w and A_n) had the different variation patterns along the Yangtze Estuary. For the D_w (or A_w) process, it includes two major steps: nitrate (NAR) and nitrite reduction (NIR) (Fig. 6). In contrast, D_n (or A_n) has two pathways. One pathway includes 4 major steps: ammonia oxidation (AO), nitrite oxidation (NIO), NAR and NIR. The other just includes 2 major steps: AO and NIR (Fig. 6). The variations of D_w and D_n (as well as A_w and A_n) in the Yangtze Estuary were mainly affected by their respective controlling factors. Redundancy analysis showed that the rates of both D_w and A_w were positively related to NO_3^- concentrations, while the rates of both D_n and A were negatively related to NO_3^- concentrations (Fig. 5). These relationships indicated that in water systems with high NO_x^- levels, bottom water can directly provide NO_x^- as substrate and electron donor for nitrogen removal microorganisms, whereas nitrogen removal microorganisms rely more on NO_x^- produced by nitrification in NO_x^- -limited water environments (Seitzinger et al., 2006).

In this study, it is also shown that the D_w and A_w rates were significantly and positively related to ferrous iron, whereas the D_n and A rates had no correlations with ferrous iron (Fig. 5). These correlations were likely dependent on the reaction pathways of different nitrogen removal processes (Fig. 6). Numerous studies implied that nitrate may be reduced to nitrite by ferrous Fe oxidation, followed by rapid reaction of nitrite to di-nitrogen gas (Postma et al., 1991; Deng et al., 2015; Yin et al., 2015). Therefore, high availability of ferrous iron would increase the rates of both D_w and A_w by stimulating the NAR. In contrast, as mentioned above, D_n (or A_n) has two pathways. Compared with the first pathway, the second pathway has fewer steps and higher conversion efficiency (Miao et al., 2018). Hence, we assumed that the second pathway was the dominant pathway of D_n (or A_n) in the sediments of the study area. Because AO might be the rate-limiting step of D_n (or A_n) and not affected by ferrous iron (Burgin and Hamilton, 2007), no correlation was observed between ferrous iron and D_n (or A_n).

In addition, we found that there was a positive correlation between OC and D_w , but OC was not correlated to D_n (Fig. 5). D_w is a heterotrophic process in which organic matter is utilized as an electron donor and carbon source (Kim, 2016). Therefore, D_w might be accelerated with increasing OC concentrations. However, AO is the first step of nitrification which is an autotrophic process and a rate-limiting step of NR_n . Hence, no significant link between OC and D_n was observed in the study area.

4.3. Key factors determining the relative importance of different nitrogen removal processes along the Yangtze Estuary

In different ecosystems, either NR_w or NR_n may play a leading role in NR. For instance, in high nitrate loading circumstances, NR was dominated by NR_w (Koopjakobsen and Giblin, 2010). However, in some paddy fields where N fertilizers used are urea and ammonium sulphate,

NR_n may represent a significant pathway of NR (Carrasco et al., 2004). In the present study, the relative importance of NR_w decreased seawards, and in contrast it increased for NR_n (Fig. 4), which might be attributed to near-bottom water nitrate concentration variation along the Yangtze Estuary. The nitrate concentrations decreased seawards, ranging from 3.31 to 138.20 μM (Table 1). It has been reported that in systems with bottom water NO_3^- concentrations less than 10 μM , D_n was the dominant denitrification pathway, while at NO_3^- concentrations more than 60 μM , D_w became the main denitrification pathway (Seitzinger et al., 2006). Our results are in agreement with the previous findings.

It is noteworthy that compared with February, the relative importance of NR_w increased, while the relative importance of NR_n decreased in July (Fig. 4). These results were likely related to DO. The concentration of DO in the Yangtze Estuary was lower in summer (about 5.32 mg L^{-1}), which was only about half of that in winter (about 10.26 mg L^{-1}). Under the hypoxic condition, the rate of oxygen uptake across the sediment-water interface and penetration depth of oxygen decreased, which was adverse to the nitrification and its coupling with denitrification and anammox (Rasmussen, 1992). Therefore, DO might be an important factor controlling the relative importance of NR_w and NR_n in the Yangtze Estuary.

In addition, there was a significant positive correlation between salinity and the ratios of NR_n to NR_w (Fig. 5). The variation of salinity was opposite to that of nitrate concentrations along the estuary (Fig. 4). Therefore, NO_3^- concentrations rather than salinity may remain the key factor determining the nitrogen removal processes in the study area. However, the previous studies conducted by Rysgaard et al. (1993) and Trimmer et al. (2006) reported that even though NO_3^- concentration was at a high level, D_n still played an important role in saltwater environments, compared with freshwater environments. Their findings were different from the viewpoint that in aquatic systems with high NO_3^- concentrations, D_w was the dominant denitrification pathway. This comparison implies that in addition to NO_3^- concentrations, salinity might also be a factor affecting the relative importance of NR_n .

As another pathway of nitrate dissimilation reduction, dissimilatory nitrate reduction to ammonium (DNRA) is an alternative NH_4^+ source for anammox (Song et al., 2016). This may be especially important in some habitats where nitrate reduction is dominated by DNRA (Dunn et al., 2013; Friedl et al., 2018). Previous studies show that DNRA accounted on average for about 26–30% of total dissimilatory nitrate reduction in the Yangtze estuarine and coastal sediments (Song et al., 2013; Deng et al., 2015). However, in this study, we ignored the effects of DNRA on anammox, so it might lead to a slight overestimation of actual anammox rates.

5. Conclusions

This study investigated the ambient rates of nitrogen removal processes (including denitrification and anammox) and their coupling with nitrification along the salinity gradient of the Yangtze Estuary. The rates of total denitrification and anammox varied between 0.44 and 7.03 $\mu\text{mol N m}^{-2} \text{h}^{-1}$ and between 0.09 and 1.21 $\mu\text{mol N m}^{-2} \text{h}^{-1}$. The rates of nitrogen removal processes coupled with nitrification ranged from below the detection limit to 4.26 $\mu\text{mol N m}^{-2} \text{h}^{-1}$ for denitrification and from below the detection limit to 0.73 $\mu\text{mol N m}^{-2} \text{h}^{-1}$ for anammox. In general, the rates of coupled nitrification-nitrogen removal processes increased seawards in the study area, which were opposite to the spatial distributions of direct denitrification and anammox rates. The coupling of nitrogen removal processes to nitrification was associated tightly with NO_3^- concentration in benthic water. However, their relative importance in total nitrogen loss depended on NO_3^- concentrations, dissolved oxygen and salinity of sampling sites.

Acknowledgements

This work was supported by the National Natural Science Foundation of China (Nos: 41725002, 41671463, 41601530, 41761144062, and 41730646). It was also supported by the Fundamental Research Funds for the Central Universities and the Chinese Ministry of Science and Technology (Nos. 2016YFA0600904, and 2016YFE0133700). We would like to thank crew of “Runjiang 1” scientific expedition vessel for their help with sample collection. Many thanks are also given to anonymous reviewers and editor for constructive comments on this manuscript. Data presented here can be obtained by sending a request to the corresponding author.

Appendix A. Supplementary data

Supplementary data to this article can be found online at <https://doi.org/10.1016/j.ecss.2019.02.043>.

References

- Aelion, C.M., Warttinger, U., 2010. Sulfide inhibition of nitrate removal in coastal sediments. *Estuar. Coasts* 33, 798–803.
- An, S., Gardner, W., 2002. Dissimilatory nitrate reduction to ammonium (DNRA) as a nitrogen link, versus denitrification as a sink in a shallow estuary (Laguna Madre/Baffin Bay, Texas). *Mar. Ecol. Prog. Ser.* 237, 41–50.
- Awata, T., Oshiki, M., Kindaichi, T., Ozaki, N., Ohashi, A., Okabe, S., 2013. Physiological characterization of an anaerobic ammonium-oxidizing bacterium belonging to the “*Candidatus scalindua*” group. *Appl. Environ. Microbiol.* 79, 4145–4148.
- Bo, L., Liao, C.H., Zhang, X.D., Chen, H.L., Wang, Q., Chen, Z.Y., Gan, X.J., Wu, J.H., Zhao, B., Ma, Z.J., 2009. *Spartina alterniflora* invasions in the Yangtze River estuary, China: an overview of current status and ecosystem effects. *Ecol. Eng.* 35, 511–520.
- Brunet, R.C., Garcia-Gil, L.J., 1996. Sulfide-induced dissimilatory nitrate reduction to ammonia in anaerobic freshwater sediments. *FEMS (Fed. Eur. Microbiol. Soc.) Microbiol. Ecol.* 21, 131–138.
- Burgin, A.J., Hamilton, S.K., 2007. Have we overemphasized the role of denitrification in aquatic ecosystems? A review of nitrate removal pathways. *Front. Ecol. Environ.* 5, 89–96.
- Carrasco, D., Fernandezvaliente, E., Ariosa, Y., Quesada, A., 2004. Measurement of coupled nitrification-denitrification in paddy fields affected by Terrazole, a nitrification inhibitor. *Biol. Fertil. Soils* 39, 186–192.
- Chamchoi, N., Nitisoravut, S., Schmidt, J.E., 2008. Inactivation of ANAMMOX communities under concurrent operation of anaerobic ammonium oxidation (ANAMMOX) and denitrification. *Bioresour. Technol.* 99, 3331–3336.
- Crowe, S.A., Canfield, D.E., Mucci, A., Sundby, B., Maranger, R., 2012. Anammox, denitrification and fixed-nitrogen removal in sediments from the Lower St. Lawrence Estuary. *Biogeochem. Discuss.* 8, 9503–9534.
- Deng, F., Hou, L., Liu, M., Zheng, Y., Yin, G., Li, X., Lin, X., Chen, F., Gao, J., Jiang, X., 2015. Dissimilatory nitrate reduction processes and associated contribution to nitrogen removal in sediments of the Yangtze Estuary. *J. Geophys. Res.: Biogeosciences* 120, 1521–1531.
- Dodla, S.K., Wang, J.J., Delaune, R.D., Cook, R.L., 2008. Denitrification potential and its relation to organic carbon quality in three coastal wetland soils. *Sci. Total Environ.* 407, 471–480.
- Dong, L.F., Smith, C.J., Papaspyrou, S., Stott, A., Osborn, A.M., Nedwell, D.B., 2009. Changes in benthic nitrification, nitrate ammonification, and anammox process rates and nitrate and nitrite reductase gene abundances along an estuarine nutrient gradient (the Colne Estuary, United Kingdom). *Appl. Environ. Microbiol.* 75, 3171–3179.
- Dunn, R.J.K., Robertson, D., Teasdale, P.R., Waltham, N.J., Welsh, D.T., 2013. Benthic metabolism and nitrogen dynamics in an urbanised tidal creek: domination of DNRA over denitrification as a nitrate reduction pathway. *Estuar. Coast Shelf Sci.* 131, 271–281.
- Falkowski, P.G., Barber, R.T., Smetacek, V., 1998. Biogeochemical controls and feedbacks on ocean primary production. *Science* 281, 200–206.
- Fernandes, S.O., Javanaud, C., Michotey, V.D., Guasco, S., Anschutz, P., Bonin, P., 2016. Coupling of bacterial nitrification with denitrification and anammox supports N removal in intertidal sediments (Arcachon Bay, France). *Estuar. Coast Shelf Sci.* 179, 39–50.
- Friedl, J., De Rosa, D., Rowlings, D.W., Grace, P.R., Müller, C., Scheer, C., 2018. Dissimilatory nitrate reduction to ammonium (DNRA), not denitrification dominates nitrate reduction in subtropical pasture soils upon rewetting. *Soil Biol. Biochem.* 125, 340–349.
- Galloway, J.N., Zhao, D., Thomson, V.E., Chang, L.H., 1996. Nitrogen mobilization in the United States of America and the Peoples Republic of China. *Atmos. Environ.* 30, 1551–1561.
- Gao, D., Li, X., Lin, X., Wu, D., Jin, B., Huang, Y., Liu, M., Chen, X., 2017. Soil dissimilatory nitrate reduction processes in the *Spartina alterniflora* invasion chronosequences of a coastal wetland of southeastern China: dynamics and environmental implications. *Plant Soil* 1–17.
- Gardner, W.S., McCarthy, M.J., 2009. Nitrogen dynamics at the sediment-water interface in shallow, sub-tropical Florida Bay: why denitrification efficiency may decrease with increased eutrophication. *Biogeochemistry* 95, 185–198.
- Hou, L., Liu, M., Carini, S.A., Gardner, W.S., 2012. Transformation and fate of nitrate near the sediment-water interface of Copano Bay. *Cont. Shelf Res.* 35, 86–94.
- Hou, L., Yin, G., Liu, M., Zhou, J., Zheng, Y., Gao, J., Zong, H., Yang, Y., Gao, L., Tong, C., 2015a. Effects of sulfamethazine on denitrification and the associated N₂O release in estuarine and coastal sediments. *Environ. Sci. Technol.* 49, 326–333.
- Hou, L., Zheng, Y., Liu, M., Gong, J., Zhang, X., Yin, G., You, L., 2013. Anaerobic ammonium oxidation (anammox) bacterial diversity, abundance, and activity in marsh sediments of the Yangtze Estuary. *J. Geophys. Res.: Biogeosciences* 118, 1237–1246.
- Hou, L., Zheng, Y., Liu, M., Li, X., Lin, X., Yin, G., Gao, J., Deng, F., Chen, F., Jiang, X., 2015b. Anaerobic ammonium oxidation and its contribution to nitrogen removal in China's coastal wetlands. *Sci. Rep.* 5, 15621.
- Jetten, M.S., Wagner, M., Fuerst, J., Van, M.L., Kuenen, G., Strous, M., 2001. Microbiology and application of the anaerobic ammonium oxidation (anammox) process. *Curr. Opin. Biotechnol.* 12, 283.
- Jha, P.K., Minagawa, M., 2013. Assessment of denitrification process in lower Ishikari river system, Japan. *Chemosphere* 93, 1726–1733.
- Jia, Z., Liu, T., Xia, X., Xia, N., 2016. Effect of particle size and composition of suspended sediment on denitrification in river water. *Sci. Total Environ.* 541, 934–940.
- Kim, H., 2016. Review of inorganic nitrogen transformations and effect of global climate change on inorganic nitrogen cycling in ocean ecosystems. *Ocean Sci. J.* 51, 159–167.
- Koopjakobsen, K., Giblin, A.E., 2010. The effect of increased nitrate loading on nitrate reduction via denitrification and DNRA in salt marsh sediments. *Limnol. Oceanogr.* 55, 789–802.
- Lin, X., Liu, M., Hou, L., Gao, D., Li, X., Lu, K., Gao, J., 2017. Nitrogen losses in sediments of the East China Sea: spatiotemporal variations, controlling factors and environmental implications. *J. Geophys. Res.: Biogeosci.* 122, 2699–2715.
- Lindsay, M.R., Webb, R.L., Strous, M., Jetten, M.S., Butler, M.K., Forde, R.J., Fuerst, J.A., 2001. Cell compartmentalisation in planctomycetes: novel types of structural organisation for the bacterial cell. *Arch. Microbiol.* 175, 413–429.
- Marks, B.M., Chambers, L., White, J.R., 2016. Effect of fluctuating salinity on potential denitrification in coastal wetland soil and sediments. *Soil Sci. Soc. Am. J.* 80, 516–526.
- McTigue, N.D., Gardner, W.S., Dunton, K.H., Hardison, A.K., 2016. Biotic and abiotic controls on co-occurring nitrogen cycling processes in shallow Arctic shelf sediments. *Nat. Commun.* 7, 13145. <https://doi.org/10.1038/ncomms>.
- Meyer, R.L., Risgaard-Petersen, N., Allen, D.E., 2005. Correlation between anammox activity and microscale distribution of nitrite in a subtropical mangrove sediment. *Appl. Environ. Microbiol.* 71, 6142–6149.
- Miao, Y., Peng, Y., Zhang, L., Li, B., Li, X., Lei, W., Wang, S., 2018. Partial nitrification-anammox (PNA) treating sewage with intermittent aeration mode: effect of influent C/N ratios. *Chem. Eng. J.* 334, 664–672.
- Minjeaud, L., Bonin, P.C., Michotey, V.D., 2008. Nitrogen fluxes from marine sediments: quantification of the associated co-occurring bacterial processes. *Biogeochemistry* 90, 141–157.
- Mulder, A., Graaf, A.A.V.D., Robertson, L.A., Kuenen, J.G., 1995. Anaerobic ammonium oxidation discovered in a denitrifying fluidized bed reactor. *FEMS (Fed. Eur. Microbiol. Soc.) Microbiol. Ecol.* 16, 177–184.
- Nielsen, L.P., 1992. Denitrification in sediment determined from nitrogen isotope pairing. *FEMS (Fed. Eur. Microbiol. Soc.) Microbiol. Ecol.* 9, 357–362.
- Paerl, H.W., Fulton, R.S., 2006. Ecology of harmful marine algae. In: Graneli, E., Turner, J. (Eds.), *Ecology of Harmful Algae*. Springer, Berlin, pp. 95–107.
- Piña-Ochoa, E., Álvarez, M., 2006. Denitrification in aquatic environments: a cross-system analysis. *Biogeochemistry* 81, 111–130.
- Postma, D., Boesen, C., Kristiansen, H., Larsen, F., 1991. Nitrate reduction in an unconfined sandy aquifer: water chemistry, reduction processes, and geochemical modeling. *Water Resour. Res.* 27, 2027–2045.
- Rasmussen, H., 1992. Microelectrode studies of seasonal oxygen uptake in a coastal sediment, role of molecular diffusion. *Mar. Ecol. Prog. Ser.* 81, 289–303.
- Risgaard-Petersen, N., Nielsen, L.P., Rysgaard, S., Dalsgaard, T., Meyer, R.L., 2003. Erratum: application of the isotope pairing technique in sediments where anammox and denitrification co-exist. *Limnol. Oceanogr. Methods* 1, 63–73.
- Roden, E., Lovley, D., 1993. Evaluation of ⁵⁵Fe as a tracer of Fe(III) reduction in aquatic sediments. *Geomicrobiol. J.* 11, 49–56.
- Rysgaard, S., Risgaard-Petersen, N., Nielsen, L.P., Revsbech, N.P., 1993. Nitrification and denitrification in lake and estuarine sediments measured by the N dilution technique and isotope pairing. *Appl. Environ. Microbiol.* 59, 2093–2098.
- Seitzinger, S., Harrison, J.A., Böhlke, J.K., Bouwman, A.F., Lowrance, R., Peterson, B., Tobias, C., Dreht, G.V., 2006. Denitrification across landscapes and waterscapes: a synthesis. *Ecol. Appl.* 16, 2064–2090.
- Senga, Y., Mochida, K., Fukumori, R., Okamoto, N., Seike, Y., 2006. N₂O accumulation in estuarine and coastal sediments: the influence of H₂S on dissimilatory nitrate reduction. *Estuar. Coast Shelf Sci.* 67, 231–238.
- Shang, Q., Yang, X., Gao, C., Wu, P., Liu, J., Xu, Y., Shen, Q., Zou, J., Guo, S., 2011. Net annual global warming potential and greenhouse gas intensity in Chinese double rice-cropping systems: a 3-year field measurement in long-term fertilizer experiments. *Glob. Chang. Biol.* 17, 2196–2210.
- Song, G.D., Liu, S.M., Marchant, H., Kuypers, M.M.M., 2013. Anaerobic ammonium oxidation, denitrification and dissimilatory nitrate reduction to ammonium in the East China Sea sediment. *Biogeochemistry* 10, 6851–6864.
- Song, G.D., Liu, S.M., Kuypers, M.M.M., Lavik, G., 2016. Application of the isotope pairing technique in sediments where anammox, denitrification, and dissimilatory nitrate reduction to ammonium coexist. *Limnol. Oceanogr. Methods* 14, 801–815.
- Strous, M., 2000. Microbiology of anaerobic ammonium oxidation. *Appl. Sci.* 12, 349–360.

- Tortell, P.D., 2005. Dissolved gas measurements in oceanic waters made by membrane inlet mass spectrometry. *Limnol Oceanogr. Methods* 3, 24–37.
- Trimmer, M., Nicholls, J.C., Deflandre, B., 2003. Anaerobic ammonium oxidation measured in sediments along the Thames estuary, United Kingdom. *Appl. Environ. Microbiol.* 69, 6447–6454.
- Trimmer, M., Risgaard-petersen, N., Nicholls, J.C., Engström, P., 2006. Direct measurement of anaerobic ammonium oxidation (anammox) and denitrification in intact sediment cores. *Aust. J. Agric. Res.* 326, 37–47.
- Xia, X., Jia, Z., Liu, T., Zhang, S., Zhang, L., 2017. Coupled nitrification-denitrification caused by suspended sediment (SPS) in rivers: importance of SPS size and composition. *Environ. Sci. Technol.* 51, 212–221.
- Yang, W., Zhao, Q., Lu, H., Ding, Z., Meng, L., Chen, G.H., 2015. Sulfide-driven autotrophic denitrification significantly reduces N₂O emissions. *Water Res.* 90, 176–184.
- Yin, G., Hou, L., Liu, M., Liu, Z., Gardner, W.S., 2014. A novel membrane inlet mass spectrometer method to measure ¹⁵NH₄⁺ for isotope-enrichment experiments in aquatic ecosystems. *Environ. Sci. Technol.* 48, 9555–9562.
- Yin, G., Hou, L., Liu, M., Zheng, Y., Li, X., Lin, X., Gao, J., Jiang, X., 2016. Effects of thiamphenicol on nitrate reduction and N₂O release in estuarine and coastal sediments. *Environ. Pollut.* 214, 265–272.
- Yin, G., Hou, L., Liu, M., Zheng, Y., Li, X., Lin, X., Gao, J., Jiang, X., Wang, R., Yu, C., 2017. Effects of multiple antibiotics exposure on denitrification process in the Yangtze Estuary sediments. *Chemosphere* 171, 118–125.
- Yin, G., Hou, L., Zong, H., Ding, P., Liu, M., Zhang, S., Cheng, X., Zhou, J., 2015. Denitrification and anaerobic ammonium oxidation across the sediment-water interface in the hypereutrophic ecosystem, Jinpu Bay, in the northeastern coast of China. *Estuar. Coasts* 38, 211–219.
- Yoshinaga, I., Amano, T., Yamagishi, T., Okada, K., Ueda, S., Sako, Y., Suwa, Y., 2011. Distribution and diversity of anaerobic ammonium oxidation (anammox) bacteria in the sediment of a eutrophic freshwater lake, Lake Kitaura, Japan. *Microb. Environ.* 26, 189–197.
- Zhao, H., Yang, W., Xia, L., Qiao, Y., Xiao, Y., Cheng, X., An, S., 2015. Nitrogen-enriched eutrophication promotes the invasion of *Spartina alterniflora* in coastal China. *Clean. - Soil, Air, Water* 43, 244–250.
- Zheng, Y., Hou, L., Newell, S., Liu, M., Zhou, J., Zhao, H., You, L., Cheng, X., 2014. Community dynamics and activity of ammonia-oxidizing prokaryotes in intertidal sediments of the Yangtze estuary. *Appl. Environ. Microbiol.* 80, 408–409.
- Zheng, Y., Hou, L., Liu, M., Newell, S., Yin, G.Y., Yu, C., Zhang, H., Li, X., Gao, D., Gao, J., Wang, R., Liu, C., 2017. Effects of silver nanoparticles on nitrification and associated nitrous oxide production in aquatic environments. *Sci. Adv.* 3 (8), e1603229.
- Zheng, Y., Jiang, X., Hou, L., Liu, M., Lin, X., Gao, J., Li, X., Yin, G., Yu, C., Wang, R., 2016. Shifts in the community structure and activity of anaerobic ammonium oxidation bacteria along an estuarine salinity gradient. *J. Geophys. Res.: Biogeosci.* 121, 1632–1645.
- Zhou, S., Borjigin, S., Riya, S., Terada, A., Hosomi, M., 2014. The relationship between anammox and denitrification in the sediment of an inland river. *Sci. Total Environ.* 490, 1029–1036.